Lifetimes of image-potential states on Cu(100) and Ag(100) measured by femtosecond time-resolved two-photon photoemission

I. L. Shumay
Max-Planck-Institut für Quantenoptik, D-85740 Garching, Germany
and Lehrstuhl für Festkörperphysik, Universität Erlangen-Nürnberg, D-91058 Erlangen, Germany

U. Höfer
Max-Planck-Institut für Quantenoptik, D-85740 Garching, Germany
and Physik Department, Technische Universität München, D-85747 Garching, Germany

Ch. Reuß, U. Thomann, W. Wallauer,* and Th. Fauster
Max-Planck-Institut für Plasmaphysik, D-85740 Garching, Germany
and Lehrstuhl für Festkörperphysik, Universität Erlangen-Nürnberg, D-91058 Erlangen, Germany
(Received 16 June 1998)

We report time-resolved studies of image-potential states on Cu(100) and Ag(100). Femtosecond ultraviolet-pump and infrared-probe techniques combined with two-photon photoemission have been used to measure relaxation dynamics of $n=1$, 2, and 3 image-potential states. We found the lifetimes of these states on Cu(100) at room temperature to be 40 ± 6, 120 ± 15, and 300 ± 20 fs, respectively. The corresponding values for Ag(100) are 55 ± 5, 160 ± 10, and 360 ± 15 fs. [S0163-1829(98)06643-0]

I. INTRODUCTION

Image-potential states are a class of near-surface states which are created by Coulombic interaction of an electron residing outside a metal surface and its image charge in the solid.[1,2] The electron is essentially trapped between the image potential on the vacuum side and the surface barrier created by a gap of available bulk electronic states in the crystal. Image-potential states form a Rydberg-type series of energy levels condensing near the vacuum level with binding energies $E_b \approx 0.85\ \mathrm{eV}/n^2$.

Because these states are normally unoccupied, image-potential states at metal surfaces were first detected and identified experimentally by inverse photoemission spectroscopy.[3–5] The first high-resolution measurements of image-potential states were made with two-photon photoemission (2PPE) on single-crystal Ag, Cu, and Ni surfaces.[6] Image-potential states up to $n=4$ have been resolved on Ag(100).[7]

Image-potential states are expected to have much longer lifetimes compared to excited bulk states. This is because image-potential states are located mainly in front of the surface, which keeps the overlap of their wave functions with bulk-state wave functions relatively small. Higher-order wave functions are located further in the vacuum, and the lifetime of the image-potential states is theoretically predicted[1] to increase as n^3. Because of their simplicity, image-potential states provide a useful model for studying the coupling of surface electronic states to the substrate in the time domain. It is this coupling that governs the cross sections and branching ratios of practically all electronically induced adsorbate reactions at metal surfaces.[8]

The lifetimes of image-potential states have been deduced from their spectral width or line shape in 2PPE spectroscopy.[9] However, the accuracy of those measurements was limited by instrumental resolution. Time-resolved 2PPE with femtosecond pulses enables a direct measurement of the image-potential-state lifetimes. In principle, the temporal resolution in this case is limited only by the available laser-pulse duration. Time-resolved studies of the image-potential states have been done on Ag(100),[10–12] Ag(111),[12] and Cu(111).[13–15] The use of femtosecond light pulses with large spectral width allows coherent excitation of several higher-order image-potential states, making quantum-beat spectroscopy of these states possible.[16]

Here we report time-resolved studies of image-potential states with $n\leqslant 3$ on Cu(100) and Ag(100). Femtosecond ultraviolet-pump and infrared-probe techniques combined with two-photon photoemission have been used to measure relaxation dynamics of $n=1$, 2, and 3 image-potential states. A high laser repetition rate, resulting in a high signal-to-noise ratio, high energy resolution, and a small acceptance angle of the spectrometer, allowed precise measurement of the lifetimes of these states.

II. EXPERIMENT

The experiments have been carried out in an ultrahigh-vacuum system at a base pressure better than 3×10^{-8} Pa at room temperature. The samples were cleaned in the usual way by neon sputtering and heating cycles. The surface quality was certified using low-energy electron diffraction and Auger spectroscopy.

The principle of the time-resolved two-photon photoemission spectroscopy of image-potential states is straightforward. For both Cu(100) and Ag(100) surfaces, the vacuum level E_{vac} lies in the middle of the sp band gap of the projected bulk band structure (Fig. 1). The UV laser pulse

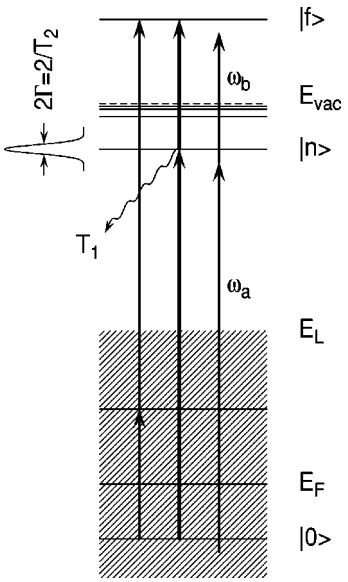

FIG. 1. Diagram of the energy levels probed by two-photon photoemission on (100) surfaces of Cu and Ag. Image-potential states form a series converging toward the vacuum level which lies in the middle of the band gap of the projected bulk band structure. E_L is the lower-energy edge of the band gap. The hatched area shows allowed bulk states. In the center, an UV laser pulse excites an electron from the bulk state $|0\rangle$ below the Fermi level E_F into an image-potential state $|n\rangle$, and an IR pulse ionizes the electron into a state $|f\rangle$ in continuum. Simultaneously, an electron can be ionized directly from the initial state via a two-photon process. The figure corresponds to excitation of the $n=1$ state. Two other processes compete with this resonant excitation: IR excitation of electrons into bulk states above the Fermi level with subsequent UV ionization (this process is shown on the left), and the off-resonant excitation of the image-potential states from other available initial states (this process is illustrated on the right).

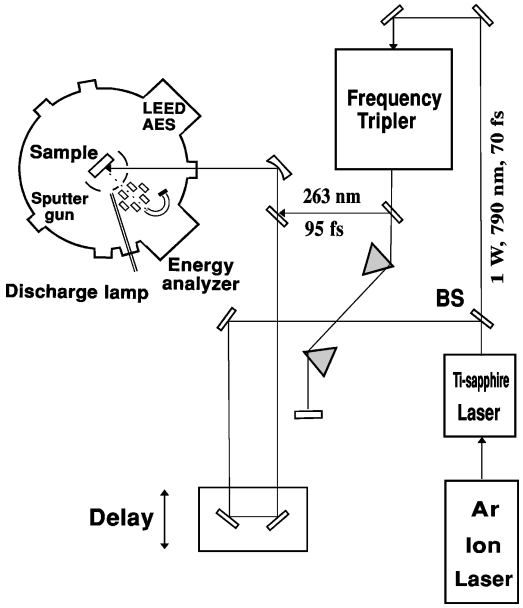

FIG. 2. Experimental arrangement.

($\hbar\omega_a$) excites electrons from the occupied state $|0\rangle$ below the Fermi energy E_F to the image-potential state $|n\rangle$ below the vacuum level. Population in the image-potential states can be probed in real time by ionizing electrons from image-potential states to states $|f\rangle$ in continuum by an IR laser pulse ($\hbar\omega_b$) which is delayed in time relative to the excitation pulse. The whole 2PPE spectrum of the image-potential states is obtained by scanning the analyzer energy while keeping the photon energies of the pump and probe pulses fixed. The laser wavelength must be tuned to have the UV photon energy lower than the sample work function $E_{vac}-E_F$ in order to suppress one-photon photoemission from states below the Fermi level. Two-color 2PPE has the advantage that intensities of the two pulses can be adjusted independently to increase the signal amplitude without inducing the space charge at the same time.[7] In addition, with two-color 2PPE one can distinguish between different competing excitation processes (see Fig. 1).

In the experiments (the experimental arrangement is shown in Fig. 2) we used a self-mode-locked Ti-sapphire laser (Tsunami, Spectra-Physics) producing a continuous train of laser pulses (pulse duration 70 fs) at a repetition rate of 82 MHz, with an average beam power of about 1.1 W. The laser beam was split into two parts. One part, containing 80% of the energy, was used to generate the third harmonic of the fundamental wavelength (Ultrafast Harmonic System, Inrad). UV light with an average power measured at the input window of an UHV chamber of about 40 mW was used as the pump beam. The UV pulse duration determined from the width of the cross-correlation function of UV and IR pulses, measured by detecting the 2PPE signal from a clean Cu(111) surface[14] as a function of the IR pulse delay, was 95 fs. The remaining part of the fundamental (IR) radiation from the laser was used to probe population of the image-potential states after variable delay. The pump (UV) and probe (IR) photon energies used in the experiments were 4.71 and 1.57 eV, respectively, for Cu(100), and 4.48 and 1.49 eV, respectively, for Ag(100). Group-velocity dispersion of the UV pulses, resulting mainly from the input window of the UHV chamber, was compensated for by an optical compressor consisting of a pair of quartz prisms. The UV and IR pulses were focused collinearly onto the sample with a 50-cm focal distance concave mirror.

With the estimated laser fluence on the sample less than 3×10^{-7} J/cm^2, we did not see any space-charge effects in the photoelectron spectra. The high repetition rate of our laser system ensured a very high dynamic range of 2PPE intensity measurements. The count rate at the peak of the $n=1$ image-potential state was of the order of 10^5 counts/s. This resulted in an unprecedented high signal-to-noise ratio in our experiments, and made possible precise lifetime measurements.

The kinetic energy of the photoemitted electrons was analyzed in a sectoral hemispherical analyzer equipped with three-lens entrance and exit electron optics. The system had an angular resolution of about $\pm0.6°$.[2] Energy resolution in the present set of measurements was about 40 meV at a pass energy of 1.2 eV. The experiments were performed at normal emission. Electrons photoemitted from the bottom of the image-potential band with nearly zero parallel momentum $k_\parallel$ have been detected.

III. RESULTS

Typical room-temperature 2PPE energy-resolved spectra of image-potential states on Cu(100), as a function of probe

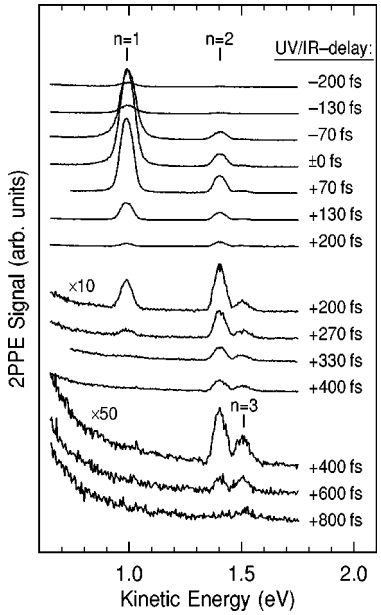

FIG. 3. Two-photon photoemission spectra from Cu(100) taken at different delays of the IR probe pulse relative to the UV pump pulse.

pulse delay, are shown in Fig. 3. The spectra show three distinct peaks corresponding to emission from the $n=1$, 2, and 3 image-potential states. One clearly sees that, as the time delay increases, the intensity of the $n=1$ state decays first. When the IR probe pulse is delayed by about 200 fs relative to the UV pump pulse, the intensity of the $n=2$ state dominates the spectrum. At even longer delays the $n=1$ state disappears completely, and the intensity of the $n=3$ state relative to that of the $n=2$ state increases, showing that the former lives longer. The signal from the $n=3$ state and its shoulder arising from $n \geqslant 4$ states persists even at probe delays as high as 800 fs. These observations are in qualitative agreement with the theoretical predictions[1] that the lifetime of image-potential states should increase as n^3. To measure the lifetime of a particular image-potential state, the energy analyzer was tuned to the desired peak in the spectrum, and the relative probe-pump delay was scanned while measuring the count rate of the photoelectrons.

The 2PPE cross-correlation traces for the $n=1$ image-potential states of Ag(100), Cu(100), and Cu(111), measured at room temperature, are shown in Fig. 4. Note that the maxima of the experimental curves showing the count rate of the detected photoelectrons as a function of the pump-probe delay are shifted to longer probe delays relative to the peak of the pump-probe correlation function. This shift reflects the lifetime of the corresponding image-potential state, and has been observed in earlier time-resolved measurements.[10–12] The shift becomes larger for image-potential states with higher quantum numbers. The transient responses have a shoulder at negative probe delays which comes from the competing process of IR excitation followed by UV ionization.

In order to deduce the lifetimes of the image-potential states, one has to know precisely the duration of both pump and probe pulses. We measured the duration of the infrared probe pulses with an optical autocorrelator based on noncollinear optical second-harmonic generation. The obtained

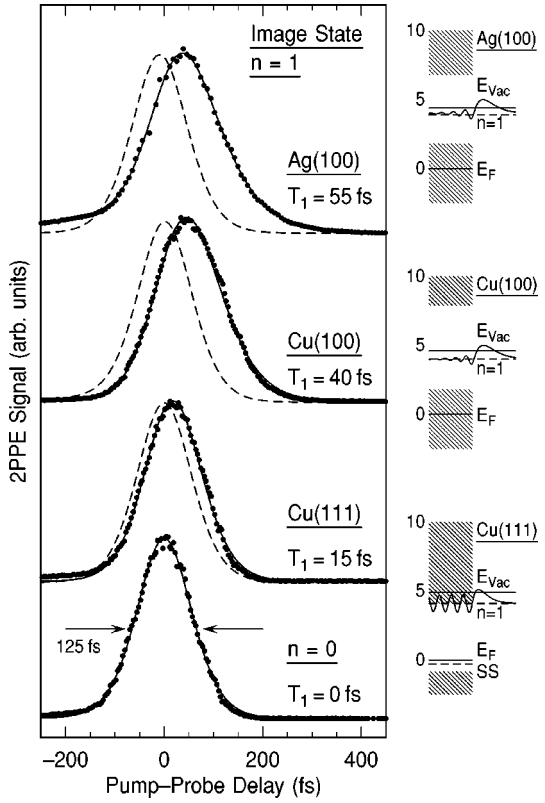

FIG. 4. Transient responses of the $n=1$ image-potential states on Ag(100), Cu(100), and Cu(111). The lower trace (also reproduced by the dashed line on the upper traces) is the pump-probe cross-correlation reference, with a width of 125 fs measured by time-resolved two-photon photoemission spectroscopy from the occupied surface state on Cu(111) in the absence of a resonant intermediate state. Also shown are the projected band structures of the corresponding surfaces with the image-potential-state wave function.

probe-pulse duration was typically about 70 fs. The duration of the UV pump pulses was obtained from the cross-correlation of the UV and IR pulses measured by time-resolved 2PPE spectroscopy from an occupied surface state on a Cu(111) sample mounted in the UHV chamber on the same holder as the sample being studied. In this case an electron is ionized from the surface state into the continuum through a virtual intermediate state which has a negligible lifetime [at the photon energies used, the image state on Cu(111) is far away from resonance with this intermediate state[17]], and the pump-probe cross-correlation trace is a measure of the UV and IR pulse duration *directly at the sample*.[14] Assuming a hyperbolic secant pulse profile for both pump and probe pulses, we deduce an UV pulse duration of 94 fs.

IV. THEORETICAL MODEL

The lifetimes of the image-potential states on clean metal surfaces, although longer than the lifetimes of electronic states in the bulk material, still lie in the femtosecond range. Thus, when using laser pulses with durations of a few tens of femtoseconds, substantial changes of the image-state population occur on the time scale of the duration of the excitation pulse. This is particularly true for lower-order image-potential states. On the other hand, quantum-beat

spectroscopy of the image-potential states[16] shows that the dephasing of the image-potential-state wave functions on clean surfaces occurs on a rather long time scale (several hundred femtoseconds). Consequently, the rate-equation approximation, assuming that the transition dipole moment follows the applied light field (or that the phase relaxation time T_2 is much shorter than the energy relaxation time T_1), does not hold, and a theoretical model of the excitation process must explicitly take into account dynamic coupling of the laser field with the transition dipole moment.[18]

This is accomplished by solving the Liouville–von Neumann equation

$$\frac{d\rho}{dt}=\frac{1}{i\hbar}[H,\rho]+\left(\frac{d\rho}{dt}\right)_{relax}, \tag{1}$$

which governs the evolution of the density matrix ρ in a three-level system including an initial (bulk) state in the valence band of the material below the Fermi level, an image-potential state, and a state in the continuum where the ionized electron is detected by the electronic energy analyzer (Fig. 1). The quantum system interacts with two laser pulses having carrier frequencies 3ω (UV pump pulse) and ω (IR probe pulse). Delay of the IR pulse is varied relative to the UV pulse. The laser pulses are assumed to have a hyperbolic secant pulse profile, and have an experimentally determined pulse duration. The excitation strength is assumed to be sufficiently low so that Rabi oscillations of the population do not affect the relaxation dynamics. This assumption is experimentally substantiated by the fact that longer-lived image-potential states demonstrate purely exponential decay after excitation (see below). Apart from scaling factors, the fit parameters of the model are the position of the signal maximum relative to the experimentally found peak of the pump-probe cross-correlation, the phenomenologically introduced energy relaxation times $T_1(n)$ and $T_1(f)$ of the intermediate and final states, and the true dephasing rates $\gamma^*(0)$, $\gamma^*(n)$, and $\gamma^*(f)$ of the states, respectively. Here we assume that the decay of the off-diagonal terms of the density matrix is governed by coefficients

$$\Gamma(ij)=\hbar/2[T_1^{-1}(i)+T_1^{-1}(j)]+\Gamma^*(ij), \tag{2}$$

with

$$\Gamma^*(ij)=\gamma^*(i)+\gamma^*(j). \tag{3}$$

We note that the availability of a continuum of initial states below the Fermi level on both Cu(100) and Ag(100), from which an electron can be excited into image-potential states, and the finite energy resolution of the electrostatic energy analyzer plays a crucial role. Indeed, at a given UV photon energy, electrons can also be excited off-resonance into an intermediate state (Fig. 1, right diagram). In this case the dynamics of the excited-state population *during* the excitation pulse is governed by the coupling dynamics of the laser field with the off-resonance driven transition dipole moment, and shows a much faster decay with a characteristic time of about $(\omega-\omega_0)^{-1}$, where ω is the frequency of light and ω_0 is the resonance frequency of the transition. Indeed, in this case the amplitude of the off-diagonal term of the density matrix oscillates with the frequency $(\omega-\omega_0)$. When this term changes sign, it starts driving the excited population down.[18] Thus, the larger the detuning, the faster the population of the excited state decays. Although the excitation probability is lower for the off-resonant excitation, our computer analysis clearly shows that, given the limited energy resolution determined by a convolution of the analyzer function with the spectral width of the probe (IR) pulse, the off-resonant contribution has a noticeable effect on the deduced lifetimes. The off-resonant excitation was taken into account by incoherently summing contributions from initial states detuned from exact resonance with the image-potential state at a given photon energy as far as twice the image-potential state linewidth. At the same time, the three-level model adequately takes into account both the step-by-step ionization through an intermediate image-potential state and the direct two-photon ionization process.[19]

We made the following further assumptions in the model: (i) we neglected both energy and phase relaxation of the final state in the continuum by setting $T_1(f)=\infty$ and $\gamma^*(f)=0$; and (ii) the phase relaxation of the initial state was found to have a small effect on the deduced lifetime of the image-potential state and was also neglected: $\gamma^*(0)=0$. The latter approximations allow one to describe the dephasing in the system with one parameter: the dephasing rate $\gamma^*(n)$ of the image-potential state.

The model does not take into account the competing process which produces photoelectrons with the same kinetic energy by two-photon excitation, where the IR pulse generates hot electrons in the bulk states above the Fermi level and these are ionized by the UV pulse (Fig. 1, left diagram). As we pointed out above, this process is responsible for the appearance of wings in the transient-response curves at negative pump-probe delays for $n=1$ and 2 image-potential states. These wings have a rather strong influence on the fitting procedure with the three-level model, and reduce the achievable precision. The discrepancy between experimental data and the theory becomes particularly large for the image-potential states on Ag(100) (see Fig. 4).

The coherent interaction of the laser field with the induced electric dipole, which affects the transient dynamics of the 2PPE signal, occurs only *during* the excitation pulse. As soon as the excitation pulse is over, the image-potential-state population starts decaying purely exponentially. The decay rate is independent of any approximations of the theoretical model or exact pulse shape, and is simply the inverse value of the image-potential-state lifetime. Consequently, if the image-potential-state population lives longer than the excitation pulse duration, one can deduce the lifetime from the exponentially decaying tail of the transient 2PPE response. This is clearly seen from Figs. 5 and 6, which show the pump-probe cross-correlation traces for the $n=1$, 2, and $n=3$ states on Cu(100) and Ag(100), respectively, on a logarithmic scale. The $n=2$ and 3 response curves have been scaled to have the same amplitude as that of the $n=1$ curve.

The high count rate of photoelectrons allows one to follow the exponential decay over several orders of magnitude, and determine the lifetimes with high precision. The deduced lifetimes are close to those obtained by using computer simulations with the above theoretical model. Thus one can use the latter for deducing shorter lifetimes by fitting the transient two-photon excitation dynamics when the exponential

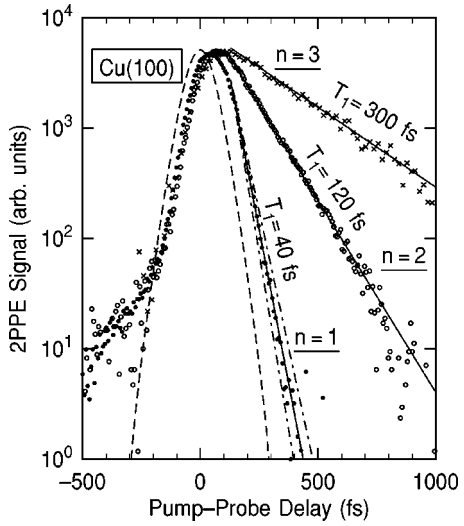

FIG. 5. Transient responses of the $n=1$, 2, and 3 image-potential states on Cu(100) on a logarithmic scale. All curves clearly show that the excited-state population decays exponentially at longer delays: solid lines correspond to exponential functions $\exp(-t/T_1)$ decaying with the corresponding lifetimes T_1. The dot-dashed lines on $n=1$ curves have a slope corresponding to a lifetime different from the best fit by ± 5 fs. The dashed line shows the pump-probe cross-correlation reference.

decay of the transient response cannot be separated reliably in time from the pump-probe cross-correlation. This is the case, for example, with the $n=1$ image-potential state on Cu(111) for which we find the lifetime of about 15 fs, in agreement with the results of Ref. 15.

In principle, one can improve the time resolution by using shorter laser pulses. However, in this case the larger spectral width of the pump pulses can lead to excitation of a coherent superposition of many quantum states,[16] and one has to model theoretically a complex transient response of the multilevel quantum system to two-photon excitation. The broader spectral width of the probe pulses results in a loss of the energy resolution, which in turn may have an effect on the decay dynamics of the transient response due to the increased contribution of the off-resonant excitation. It follows from this discussion that the femtosecond time-resolved 2PPE spectroscopy, as well as any other spectroscopic technique with ultrashort light pulses, has intrinsic limits: better time resolution always means a loss of resolution in energy.

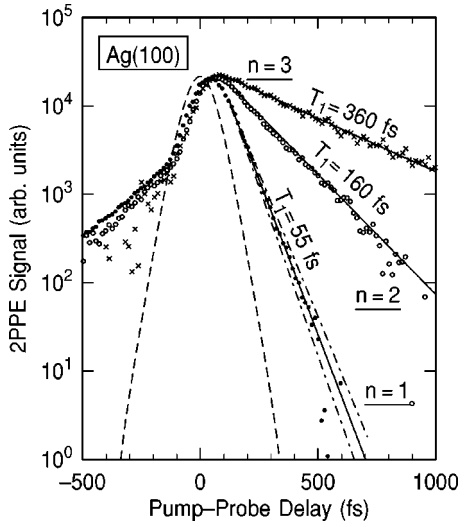

FIG. 6. Transient responses of the $n=1$, 2, and 3 image-potential states on Ag(100) on a logarithmic scale. Solid lines correspond to exponential functions $\exp(-t/T_1)$ decaying with the corresponding lifetimes T_1. The dot-dashed lines on the $n=1$ curves have a slope corresponding to the lifetime different from the best fit by ± 5 fs. The dashed line shows the pump-probe cross-correlation reference.

The transient response curves on Ag(100) ($n=1$ and 2) and Cu(100) ($n=1$) show an exponential slope at *negative* probe-pulse delays. This tail comes from hot electrons excited by the IR probe pulse into the bulk states above the Fermi level (Fig. 1), and then ionized by the UV pump pulse. The decay of this signal reflects relaxation dynamics of the photoexcited nonequilibrium electron distribution, and has been studied on single-crystal metals with different surface orientation.[13,20–22] By fitting the tails with a single-exponential function, we deduce the hot-electron lifetimes for Ag(100) to be 190 fs at $E-E_F=0.90$ eV (the energy of the intermediate state in the IR-pump and UV-probe 2PPE processes, producing electrons with the same kinetic energy as those ionized through the $n=1$ image-potential state) and 145 fs at $E-E_F=1.27$ eV (this lifetime was measured at the position of the $n=2$ image-potential state in the 2PPE spectrum). On Cu(100) we find a lifetime of 200 fs for hot electrons excited to states 1.01 eV above the Fermi level (measured at the position of the $n=1$ image-potential state in the 2PPE spectrum). Our data are in agreement with extrapolation of the data on lifetimes of hot electrons measured in Ref. 21 at higher energies above E_F.

V. DISCUSSION

The lifetimes of the image-potential states are governed by the overlap of their wave function with those of the bulk states. This explains the difference of lifetimes of the $n=1$ image-potential states on Cu(100) and Cu(111) surfaces (Fig. 4). On Cu(111) the $n=1$ image-potential state lies at the upper edge of the band gap. Thus the image-potential-state wave function decays weakly into the bulk, and its strong overlap with the wave functions of bulk states gives rise to a short lifetime. In contrast, on Cu(100) and Ag(100) the image-potential states lie close to the middle of the band gap and their wave functions are strongly damped, resulting in smaller overlap with bulk states and longer lifetimes.

The theory[1] predicts that the lifetimes of the image-potential states should increase with the state quantum number as $(n+a)^3$, where a is the quantum defect related to the phase of the wave function at the surface. The quantum defect a is 0 at the top of the band gap, and reaches its maximum value of $\frac{1}{2}$ at the bottom. The energies of the image-potential states are given by

$$E(n)=E_{vac}-0.85\text{eV}/(n+a)^2, \quad n=1,2,\ldots . \tag{4}$$

In both Cu(100) and Ag(100) the vacuum level lies near the middle of the band gap. The value of the quantum defect can be deduced from the binding energy of the $n=1$ image-potential state. We find $a=0.21$ for Cu(100) and $a=0.26$ for Ag(100), in agreement with earlier measurements.[7]

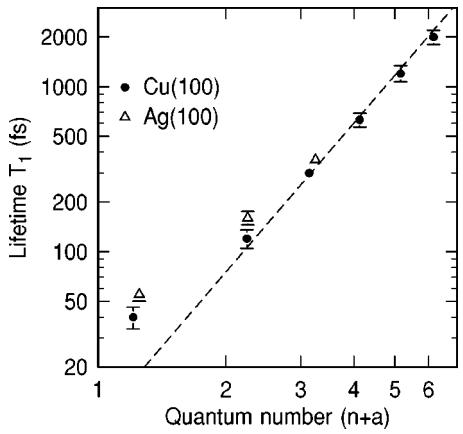

FIG. 7. Comparison of the measured image-potential lifetimes on Cu(100) and Ag(100) with the theoretical model of Ref. 1, predicting n^3 dependence.

However, experimentally measured energy spacing of the image-potential states in series (4) cannot be fitted with one value of the quantum defect a. The quantum-beat spectroscopy of the higher-order image-potential states[16] allows a precise measurement of energy spacing of states in series (4) from their beat frequencies. Thus, on Cu(100), we measured[23] quantum-beat periods $T_{34}=h/(E_4-E_3)=114$ fs, $T_{45}=h/(E_5-E_4)=230$ fs, and $T_{56}=h/(E_6-E_5)=430$ fs for successive pairs of image-potential states between $n=3$ and 6. The values of the quantum defect describing the measured energy spacings between these image-potential states lie in the range 0.15 ± 0.02, substantially lower than the theoretical value $(a=0.25)$[2] and the value giving correct binding energy ($E_1=0.57$ eV) of the $n=1$ state on Cu(100). The quantum defect giving the experimentally measured binding energy of the $n=2$ state on Cu(100) is $a=0.24$. This deviation is related to the details of the electronic structure of the surface.[2]

The lifetimes we measured on Cu(100) at room temperature are 40 ± 4, 120 ± 10, and 300 ± 20 fs, for $n=1$, 2, and 3, respectively. Similarly, on Ag(100) at room temperature we find lifetimes of 55 ± 5, 150 ± 10, and 360 ± 15 fs for $n=1$, 2, and 3 image-potential states, respectively.

In Fig. 7 we compare the experimentally measured lifetimes of the image-potential states on Cu(100) and Ag(100) with the power law n^3. The experimental points are plotted with the corresponding quantum defect values found experimentally. Also shown in Fig. 7 are the lifetimes of higher-order states ($n=4$, 5, and 6) on Cu(100) which have been measured by using coherent quantum-beat spectroscopy.[16] It is seen that the lifetimes of $n=1$ and 2 image-potential states on Ag(100), and the $n=1$ state on Cu(100), deviate significantly from the straight line in Fig. 7, corresponding to the power-law dependence n^3. However, the lifetimes of image-potential states on Cu(100) scale with the third-power law remarkably well, beginning with the $n=2$ state, whereas the theory based on many-body self-energy formalism[24] predicts a power-law dependence for states with $n\geqslant5$.

Chulkov, Silkin, and Echenique[25] calculated the binding energies and lifetimes of the image-potential states on Cu(100) and Ag(100) surfaces by using a model potential accurately reproducing the width and position of the energy gap at $k_\parallel=0$ and energies of the surface states. This model potential accurately reproduces the wave functions of the image-potential states. Within the heuristic approximation[2] the linewidth of an image-potential state is given by $\Gamma(E_n)=p_n\Gamma_b(E_n)$, where p_n is the penetration of the nth image-potential-state wave function into the bulk, and $\Gamma_b(E_n)$ is the linewidth of the bulk state at the energy E_n. Assuming a linear dependence of the linewidth of the bulk states on energy relative to the Fermi level, the lifetimes of the $n=1$ and 2 image-potential states come out to be 25.5 and 132 fs on Cu(100), and 26.5 and 132 fs on Ag(100), respectively.[25] A more detailed analysis of different contributions to the quasiparticle damping results in a better agreement of theory with the experiment for Cu(100): recent calculations[26] give the lifetimes of 30, 132, and 367 fs for $n=1$, 2, and 3 image-potential states, respectively. In Table I we compare available theoretical and experimental data for the lifetimes of the image-potential states on Cu(100) and Ag(100).

TABLE I. Lifetimes of the image-potential states on Cu(100) and Ag(100) surfaces (fs).

		Experiment	Experiment, $\hbar/\Gamma$	Theory
Cu(100)	$n=1$	40 ± 6[a]	24 ± 5[b]	30[c]
	$n=2$	120 ± 15[a]		132[c]
	$n=3$	300 ± 20[a]		367[c]
Ag(100)	$n=1$	55 ± 5[a]	31 ± 6[d]	26.5[e]
		25 ± 10[f]		
	$n=2$	160 ± 10[a]	$\geqslant66$[d]	132[e]
		180 ± 20[f]		
	$n=3$	360 ± 15[a]		

[a]This work.
[b]Reference 2.
[c]Reference 26.
[d]Reference 7.
[e]Reference 25.
[f]Reference 11.

Experimentally, the lifetimes of the low-n image-potential states have been deduced previously from energy-resolved 2PPE spectra on Cu(100) (Ref. 2) and Ag(100),[7] and from femtosecond time-resolved 2PPE on Ag(100).[10–12] The intrinsic linewidth Γ could be measured reliably only for $n=1$ and 2 states because of limited energy resolution of the energy analyzer. It was found that the intrinsic linewidth of the $n=1$ state on Cu(100) is 28 ± 6 meV, and the linewidths on $n=1$ and 2 states on Ag(100) are 21 ± 4 and 5 ± 5 meV, respectively. Assuming that the intrinsic linewidth is governed only by energy relaxation processes, this would correspond to the lifetime of 24 ± 5 fs for $n=1$ state on Cu(100), and to the lifetime of 31 ± 6 fs for $n=1$ state on Ag(100). We included these values in Table I. No reliable lifetime could be deduced from energy-resolved spectrum for $n=2$ state because of insufficient energy resolution. However, an intrinsic linewidth of 5 meV would give a lifetime of 132 fs, and the lower limit for the lifetime of the $n=2$ state on Ag(100), based on intrinsic linewidth measurements, is 66 fs.

On both Cu(100) and Ag(100), our time-resolved measurements yield longer lifetimes. However, when comparing time-resolved data with those obtained from the energy-

resolved spectra, one should take into account that the intrinsic linewidths of the image-potential peaks in 2PPE spectra is governed not only by energy (population) relaxation but also by phase-relaxation processes. Within the approximations we made in the theoretical model, the full width at half maximum 2Γ of the spectrum is related to the image-potential-state lifetime T_1 as $2\Gamma/\hbar = 1/T_1 + 2/T_2^*$ where T_2^* is the true dephasing time ($T_2^* = \hbar/\gamma^*$). The energy-relaxation time T_1 can be deduced by fitting the cross-correlation traces in time-resolved spectra (the effect of dephasing is rather small). Then, from the above formula, one finds the dephasing time. Thus we find $T_2^* = 120$ fs for the $n=1$ state on Cu(100). Similarly, $T_2^* = 140$ fs for the $n=1$ state on Ag(100). This finding proves our earlier statement that a slow dephasing of the image-potential states does not allow one to use the rate-equation approximation when describing the excitation dynamics.

We note that we have obtained the above estimates from the energy-resolved spectra measured with a nanosecond laser source. One can measure spectra with a femtosecond laser as well. However, in this case the width of the image-potential peaks in the spectrum is a function of the delay between pump and probe pulses: the spectral bandwidth is larger when pump and probe pulses overlap in time, and becomes narrower when the two pulses are well separated with an IR pulse delayed relative to the UV pulse. This change in the bandwidth of the energy-resolved spectral lines as a function of probe-pulse delay is larger for shorter laser pulses. A similar effect was observed by Hertel *et al.*[27] on Cu(111). Schoenlein *et al.*[12] also saw spectral narrowing as a function of probe delay on Ag(100). However, they explained the spectrum narrowing as due to a contribution of electrons with parallel momentum which supposedly have a shorter lifetime relaxing to the bottom of the image-potential band. In our measurements the collection angle of the energy analyzer was $\simeq 0.6°$, compared to that of 12° in Ref. 12. Thus we can neglect spectral contributions from electrons with transverse momentum.

We attribute the observed linewidth narrowing to the interplay between the step-by-step one-photon ionization through an intermediate state and the direct two-photon ionization.[19] The latter contributes a peak in the spectrum with the width depending on the T_2 time of the initial state as well as spectral widths of both the pump and the probe laser pulses. The direct two-photon process is effective only when the two laser pulses overlap. As soon as they the probe pulse is decoupled from the pump pulse at longer delays only the step-by-step process contributes to the spectrum and provides information on the exponential decay of the intermediate state population. Broader spectral width at zero delay is thus a manifestation of short T_2 time of the initial state. Such behavior of the 2PPE spectral bandwidth of the image-potential peaks as a function of the probe-pulse delay is predicted by the three-level theoretical model described above. Note that the bandwidth of the $n=0$ state on Cu(111) is delay independent, which is what one could expect by taking into account the lack of a resonant intermediate state in the 2PPE process.

Consequently, with femtosecond laser sources the correct intrinsic bandwidths in energy-resolved spectra can be deduced from spectra taken at sufficiently large positive (IR probe after UV pump) delays. With this in mind, we have measured the intrinsic linewidth of the $n=1$ state on Cu(100). Taking into account the spectral shape of the laser pulses, our value for the intrinsic linewidth for the $n=1$ image-potential state on Cu(100) agrees with earlier measurements.[17]

Schoenlein *et al.*[10–12] measured the lifetimes of $n=1$ and 2 states on Ag(100) by femtosecond time-resolved 2PPE spectroscopy. They reported lifetimes of 25 ± 10 fs for the $n=1$ state and 180 ± 20 fs for the $n=2$ state. Obviously, there is a noticeable difference from our results: we measure a substantially *longer* lifetime for the $n=1$ state (55 ± 5 fs), and a *shorter* lifetime for the $n=2$ state (160 ± 10 fs). Whereas the low count rate in earlier measurements and sample preparation procedures might have caused a discrepancy in the value of the lifetime measured for the $n=1$ state, we argue that the insufficient energy resolution of the analyzer (~ 180 meV) in Ref. 11 may account for the longer measured lifetime of the $n=2$ state. Indeed, the energy spacing between $n=2$ and 3 states on Ag(100) is about 87 meV.[7] Thus, when measuring the lifetime of the $n=2$ state, the authors of Ref. 11 could also see a contribution from the $n=3$ state which lives much longer.

Comparison of data in Table I shows that theory[25,26] predicts shorter lifetimes for $n=1$ states on both Cu(100) and Ag(100) surfaces. Agreement between theory and experiment is rather good for $n=2$ states.

VI. CONCLUSION

The transient dynamics of the $n=1$, 2, and 3 image-potential states on Cu(100) and Ag(100) have been investigated using the femtosecond pump-probe technique combined with the two-photon photoemission spectroscopy. The high repetition rate of the laser system enabled orders of magnitude improvement in the signal-to-noise ratio in our data compared to earlier measurements, and made possible reliable measurements of the image-potential states' lifetimes.

By theoretically fitting the experimental data within the framework of the density-matrix formalism in the three-level system, we were able to deduce the lifetimes of these states. On Cu(100) at room temperature we find the lifetimes to be $40\pm6, 120\pm15$, and 300 ± 20 fs, respectively. Similar measurements on Ag(100) give the lifetimes of $55\pm5, 160\pm10$, and 360 ± 15 fs for $n=1$, 2, and 3 image-potential states, respectively. We argue that the lifetimes of the longer-living higher-order states can be deduced straightforwardly from the exponentially decaying tail of the transient response, independently of the theoretical model for the excitation and ionization dynamics of the image-potential states.

Our results show that the lifetimes follow a predicted third-power law $(n+a)^3$ very well, beginning with the $n=3$ state. States with a lower quantum number deviate substantially from the power-law dependence. We attribute this discrepancy to the details of the electronic band structure of the surfaces studied.

ACKNOWLEDGMENTS

Stimulating discussions with K.-L. Kompa, M. Weinelt, and M. Kutschera are gratefully acknowledged. This research has been partially supported by the Deutsche Forschungsgemeinschaft through Grant No. SFB 338.

*Present address: Siemens AG, P.O. Box 801709, D-81617 Munich.

[1] P. M. Echenique and J. B. Pendry, J. Phys. C **11**, 2065 (1978).

[2] Th. Fauster and W. Steinmann, in *Photonic Probes of Surfaces*, edited by P. Halevi, Electromagnetic Waves: Recent Developments in Research, Vol. 2 (North-Holland, Amsterdam, 1995), Chap. 8, p. 347.

[3] P. D. Johnson and N. V. Smith, Phys. Rev. B **27**, 2527 (1983).

[4] V. Dose, W. Altmann, A. Goldmann, U. Kolac, and J. Rogozik, Phys. Rev. Lett. **52**, 1919 (1984).

[5] D. Straub and F. J. Himpsel, Phys. Rev. B **33**, 2256 (1986).

[6] K. Giesen, F. Hage, F. J. Himpsel, H. J. Rieß, and W. Steinmann, Phys. Rev. Lett. **55**, 300 (1985).

[7] S. Schuppler, N. Fischer, Th. Fauster, and W. Steinmann, Appl. Phys. A: Solids Surf. **51**, 322 (1990).

[8] W. Plummer, Science **277**, 1447 (1997).

[9] S. Schuppler, N. Fischer, Th. Fauster, and W. Steinmann, Phys. Rev. B **46**, 13 539 (1992).

[10] R. W. Schoenlein, J. G. Fujimoto, G. L. Eesley, and T. W. Capehart, Phys. Rev. Lett. **61**, 2596 (1988).

[11] R. W. Schoenlein, J. G. Fujimoto, G. L. Eesley, and T. W. Capehart, Phys. Rev. B **41**, 5436 (1990).

[12] R. W. Schoenlein, J. G. Fujimoto, G. L. Eesley, and T. W. Capehart, Phys. Rev. B **43**, 4688 (1991).

[13] T. Hertel, E. Knoesel, M. Wolf, and G. Ertl, Phys. Rev. Lett. **76**, 535 (1996).

[14] E. Knoesel, T. Hertel, M. Wolf, and G. Ertl, Chem. Phys. Lett. **240**, 409 (1995).

[15] M. Wolf, E. Knoesel, and T. Hertel, Phys. Rev. B **54**, 5295 (1996).

[16] U. Höfer, I. L. Shumay, Ch. Reuß, U. Thomann, W. Wallauer, and Th. Fauster, Science **277**, 1480 (1997).

[17] W. Wallauer and Th. Fauster, Surf. Sci. **374**, 44 (1997).

[18] R. Loudon, *The Quantum Theory of Light* (Oxford University Press, New York, 1983).

[19] V. P. Chebotayev, in *High-Resolution Laser Spectroscopy*, edited by K. Shimoda (Springer-Verlag, Berlin, 1976).

[20] M. Aeschlimann, M. Bauer, and S. Pawlik, Chem. Phys. **205**, 127 (1996).

[21] S. Ogawa, H. Nagano, and H. Petek, Phys. Rev. B **55**, 10 869 (1997).

[22] E. Knoesel, A. Hotzel, and M. Wolf, Phys. Rev. B **57**, 12 812 (1998).

[23] U. Höfer, I. L. Shumay, Ch. Reuß, U. Thomann, and Th. Fauster, Proc. SPIE **3272**, 211 (1998).

[24] P. L. de Andres, P. M. Echenique, and F. Flores, Phys. Rev. B **39**, 10 356 (1989).

[25] E. V. Chulkov, V. M. Silkin, and P. M. Echenique, Surf. Sci. Lett. **391**, L1217 (1997).

[26] E. V Chulkov, I. Sarria, V. M. Silkin, J. M. Pitarke, and P. M. Echenique, Phys. Rev. Lett. **80**, 4947 (1998).

[27] T. Hertel, E. Knoesel, A. Hotzel, M. Wolf, and G. Ertl, J. Vac. Sci. Technol. A **15**, 1503 (1997).